J Ginseng Res 43 (2019) 606–617

Contents lists available at ScienceDirect

Journal of Ginseng Research

journal homepage: http://www.ginsengres.org

Research Article

Hepatoprotective effect of ultrasonicated ginseng berry extract on a rat mild bile duct ligation model

Yoonjin Nam [1], Sung Kwon Ko [2], Uy Dong Sohn [1,*]

[1] Department of Pharmacology, College of Pharmacy, Chung-Ang University, Seoul, Korea
[2] Department of Oriental Medical Food & Nutrition, Semyung University, Chungbuk, Korea

ARTICLE INFO

Article history:
Received 1 February 2018
Received in Revised form
27 April 2018
Accepted 17 July 2018
Available online 10 August 2018

Keywords:
Acute liver failure
Ginseng berry
Hepatotoxicity
Ultrasonication
Toll-like receptor 4

ABSTRACT

Background: The *Panax ginseng* berry extract (GBE) is well known to have an antidiabetic effect. The aim of this study is to evaluate and investigate the protective effect of ultrasonication-processed *P. ginseng* berry extract (UGBE) compared with GBE on liver fibrosis induced by mild bile duct ligation (MBDL) model in rats. After ultrasonication process, the composition ratio of ginsenoside in GBE was changed. The component ratio of ginsenosides Rh1, Rh4, Rg2, Rg3, Rk1, Rk3, and F4 in the extract was elevated.
Methods: In this study, the protective effect of the newly developed UGBE was evaluated on hepatotoxicity and neuronal damage in MBDL model. Silymarin (150 mg/kg) was used for positive control. UGBE (100 mg/kg, 250 mg/kg, 500 mg/kg), GBE (250 mg/kg), and silymarin (150 mg/kg) were orally administered for 6 weeks after MBDL surgery.
Results: The MBDL surgery induced severe hepatotoxicity that leads to liver inflammation in rats. Also, the serum ammonia level was increased by MBDL surgery. However, the liver dysfunction of MBDL surgery–operated rats was attenuated by UGBE treatment via myeloid differentiation factor 88-dependent Toll-like receptor 4 signaling pathways.
Conclusion: UGBE has a protective effect on liver fibrosis induced by MBDL in rats through inhibition of the TLR4 signaling pathway in liver.

1. Introduction

Liver fibrosis is resulted from the excessive production and progressive accumulation of extracellular matrix protein, which results from chronic liver damage [1,2]. It can be caused by multiple reasons such as drugs, disease (hepatitis), autoimmune response, and toxicants [3,4]. Chronic liver damage results in the dysfunction of liver cell, which causes the accumulation of ammonia [5]. If theses conditions persist, it can develop into liver cirrhosis, hepatic encephalopathy (HE), and hepatocellular carcinoma [6,7]. Currently, lactulose is mainly used to reduce HE-related symptoms [8]. Lactulose is nonabsorbable disaccharide that acidifies gut lumen through biodegradation and reduces ammonia production from gut bacteria [9]. Lactulose is a strong laxative that frequently induces diarrhea as a side effect [10]. Therefore, it is necessary to study a new agent that restores liver function fundamentally with lower side effect.

The pathophysiological conditions are highly related to the inflammation [11]. Several studies have investigated the links between inflammatory liver injury and liver fibrosis [12,13]. As a result, pathogens such as lipopolysaccharide have been proven to play an important role in this progress of inflammation [14]. Lactulose is a well-known treatment option for HE condition.

Most pathogens are recognized by specific receptor such as toll-like receptors on the basis of particular molecular patterns [15]. Especially, toll-like receptor 4 (TLR4) plays an important role in the proinflammatory response by producing proinflammatory cytokines by upregulating nuclear factor–kappa B (NF-κB) nuclear translocation [16]. This TLR4-related inflammatory response is mediated by specific adapter protein, myeloid differentiation primary response gene 88 (Myd88) [17]. Lipopolysaccharide, an endotoxin found in the outer membranes of gram-negative bacteria, is the main ligand of TLR4 that elicits an innate immune response [18]. Bile duct ligation (BDL) surgery often leads to

* Corresponding author. Department of Pharmacology, College of Pharmacy, Chung-Ang University, 84 Heukseok-RO, Dongjak-Gu, Seoul, 06974, Republic of Korea.
E-mail address: udsohn@cau.ac.kr (U.D. Sohn).

https://doi.org/10.1016/j.jgr.2018.07.007
p1226-8453 e2093-4947/$ – see front matter

bacterial translocation of intestinal endotoxin that initiates the Myd88-dependent TLR4 signaling pathway and inflammatory responses and oxidative stress in biliary obstruction condition [19].

Since hepatic inflammation and liver fibrosis are very common diseases in humans, various animal experiment models have been established in the past decades, which can lead to inflammatory liver injury and acute liver failure [20,21]. One of the well-known models for liver inflammation is the BDL model. The ligation of common bile ducts can induce severe hepatic damage due to the excessive storage of bile acid in the liver [22]. Under BDL surgery, most animals experience severe liver injury such as liver fibrosis with morphological changes. BDL surgery is a widely accepted and used model that induces chronic liver disease in rats [23]. Sometimes, mild BDL (MBDL) surgery is applicable for long-term survival of rats and less-severity in liver damage [24,25].

Panax Ginseng Meyer (*P. ginseng*) is one of the most widely used medicinal herbs that has a long medicinal history in East Asia [26]. It is well known to have beneficial effects on obesity, cardiac- and liver-associated diseases [27–29]. The representative compounds that contribute to these beneficial effects are ginsenosides [30–32]. Ginsenosides are class of natural product steroid glycosides and triterpene saponins [33]. Ginsenosides are dispersed in the roots, berries, and leafs of *P. ginseng* [34]. Ginsenosides Rb1, Rg1, Rc, Re, and Rd are the most common compounds identified among approximately 40 known ginsenosides [35,36].

Because of diverse physiological effects of *P. ginseng*, the root and leaf part of *P. ginseng* is widely used as crude drugs or functional foods [37,38]. Many biochemical and medicinal studies have been conducted for scientific explanation of the efficacy of ginsenoside. By contrast, no systematic studies have been conducted on ginsenosides of different parts, including *P. ginseng* berry [39]. *P. ginseng* berry, which is mainly used for cultivation of *P. ginseng*, is discarded after removal of seeds. However, recent studies showed that *P. ginseng* berry has antidiabetic and antiobesity effects that may be derived from its major compound, ginsenoside Re [30].

In this study, the hepatoprotective effect of the ultrasonication-processed *P. ginseng* berry extract (UGBE) on MBDL-induced inflammatory liver injury and liver fibrosis was investigated. UGBE was made by new ultrasonication procedure from *P. ginseng* berry extract (GBE). The GBE was ultrasonicated to produce less-polar active ginsenosides in a time-efficient and cost-effective way. Liver inflammation, oxidative stress, and liver dysfunction were measured followed by MBDL surgery in rats.

2. Materials and methods

2.1. Materials

The aspartate aminotransferase (AST), alanine transaminase (ALT), glutathione peroxidase (GPx), catalase (CAT), superoxide dismutase (SOD) activity, nitric oxide (NO) assay, and tumor necrosis factor-alpha (TNF-α) enzyme-linked immunosorbent assay (ELISA) kits were purchased from BioVision, Inc. (San Francisco, US). The inducible nitric oxide synthase (iNOS) and p65 nuclear factor–kappa B (NF-κB) ELISA kit were purchased from CUSABIO (Wuhan, CN). The heme oxygenase-1 (HO-1) ELISA kit was purchased from Enzo Life Sciences, Inc. (New York, USA). The anti-TLR4 antibody, anti-Myd88 antibody, and ammonia assay kit were purchased from Abcam (Cambridge, UK). The TLR4 ELISA kit was purchased from MyBioSource (San Diego, US). The GBE and UGBE were kindly provided by Prof. S.K.K., Semyung University (Jecheon, KO). Ginsenoside standards were purchased from ChromaDex (Irvine, US). Dulbecco's phosphate buffered saline (PBS) was purchased from Welgene, Inc. (Seoul, KO). Other essential materials were purchased from Sigma-Aldrich Co., LLC (St. Louis, US).

2.2. Preparation of UGBE

Four-year grown *P. ginseng* berry was dried and added with 2000 mL ethyl alcohol per 200 g of dried *P. ginseng* berry product. The GBE was produced from *P. ginseng* berry-ethyl alcohol mixture after 2-time reflux extraction and filtration followed by being concentrated by vacuum evaporation. Then, GBE was put in an ultrasonicator (KODO, Hwaseong, KO) with an oscillation and vibration of 600 W at 100℃ and treated for 10 hrs. The remaining solutions were concentrated by vacuum evaporation and freeze-dried to obtain a brownish extract (UGBE).

For further analysis of UGBE and GBE, 2 g of each extract was extracted with 50 mL diethyl ether three times by using an ultrasonicator (KODO, Hwaseong, KO) followed by removal of supernatant. The residue was treated with 50 mL n-butanol three ties again. n-Butanol fraction that built up in the ultrasonicator was filtered and concentrated by a vacuum evaporator.

2.3. Analysis of ginsenosides in UGBE

The total ginsenoside content and ginsenoside composition of UGBE and GBE were analyzed using a Waters 1525 binary high-performance liquid chromatography (HPLC) system (Milford, US). The separation of UGBE was performed on an Eurospher analytical column (100-5 C18, 250 mm × 3.0 mm, 5 μm, Knauer, Berlin, DE) by gradient elution at room temperature. The eluent was a mixture of A (acetonitrile for HPLC) and B (distilled water for HPLC). The process of elution was carried out according to the following conditions: 0 mins, 17% of A; 25 mins, 25% of A; 50 mins, 40% of A; 105 mins, 60% of A; 110 mins, 100% of A. The flow rate was 0.8 mL/min, the injection volume was 20 μL, and the chromatograms were obtained using a Ultraviolet-visible Waters 2478 Dual λ Absorbance Detector (Milford, USA) at 203 nm.

2.4. MBDL model

Since complete ligation of all bile ducts leads to death in a few weeks, MBDL surgery was performed on rats to evaluate the long-term effect of UGBE [40]. Rats underwent mild bile duct ligation surgery, in which only 3 out of 5 bile ducts were ligated after midline ventral incision, under diethyl-ether anesthesia. The ligature was placed between three upper bile ducts (proximal) and two bottom bile ducts (distal) portion of the rest of bile duct. Nonabsorbable surgical suture materials were used for ligations. In sham-operation group, a midline incision was performed without MBDL surgery. Midline suture was performed with same materials used in MBDL surgeries. All animals recovered from operation with antibiotic drugs (ointment) and warm condition for 1 wk. The MBDL surgery is summarized in Fig. 1.

2.5. Experimental design

Seventy-two male Sprague-Dawley rats (200-250 g) were purchased from Samtako Bio Korea (Osan, Korea). The animals were group-housed in cages with wire-net floors in a room controlled for temperature (24-25°C) and humidity (70-75%) and were fed a normal laboratory diet from Samtako Bio Korea. All animals were fasted for 24 hrs before surgery and sacrifice but were allowed free access to tap water. Animal experiments were approved by the Institutional Animal Care and Use Committee (IACUC) of Chung-Ang University, in accordance with the guide for the Care and Use of Laboratory Animals in Seoul, Korea (CAUIACUC-2016-00095).

All rats were randomly divided into the following eight groups and fed an appropriate reagent or extract for 6 wks (n = 9); (a)

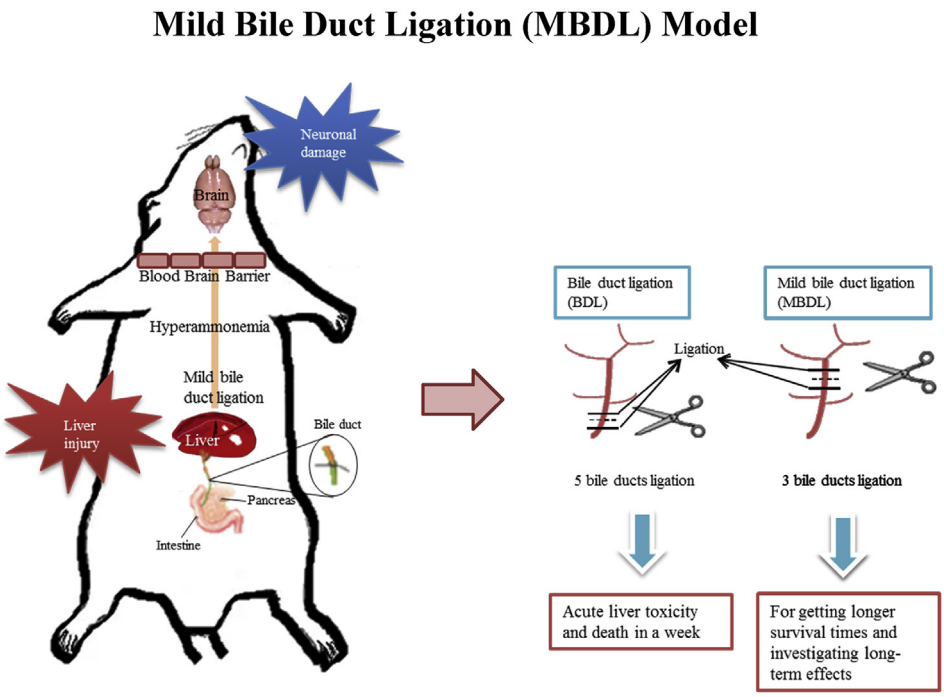

Fig. 1. The graphical summary of mild bile duct ligation model. The mild bile duct ligation model was performed to induce hepatic encephalopathy in rats instead of bile duct ligation model. Rats underwent ligation surgery, in which only 3 out of 5 bile ducts were ligated after midline ventral incision for long-term survival.

control group, 2 mL/kg (b.w.) of normal saline (p.o.); (b) sham-operation group, 2 mL/kg (b.w.) of normal saline (p.o.); (c) MBDL group, 2 mL/kg (b.w.) of normal saline (p.o.); (d) GBE group, 250 mg/kg (b.w.) of GBE (p.o.); (e) silymarin group, 250 mg/kg (b.w.) of silymarin (p.o.); (f) UGBE1 group, 100 mg/kg (b.w.) of UGBE (p.o.); (g) UGBE 2 group, 250 mg/kg (b.w.) of UGBE (p.o.); (h) UGBE3 group, 500 mg/kg (b.w.) of UGBE (p.o.). All rats underwent MBDL surgery except control and sham-operation groups. Twenty-four hours after the last administration, all rats were sacrificed by cervical dislocation. The blood and liver were removed immediately. All collected samples were properly handled for further assays.

2.6. Preparation and biochemical assays of liver and serum samples

After being sacrificed, whole blood samples (4–5 mL) were collected from rat inferior vena cava. Whole blood samples were collected in SST II Plus plastic serum tube (Becton, Dickinson, and Company, US). Collected samples were centrifuged at 10,000 g, 4°C for 20 mins. After being centrifuged, serum samples were obtained and immediately flash-frozen at −80°C for further assays (AST, ALT, and ammonia level).

Liver samples were perfused with PBS (pH 7.4) solution through the portal vein to remove any red blood cells. The portal vein was cannulated with a 23-gauge I.V. catheter (Korean vaccine, KO), and the abdominal inferior vena cava was cut immediately. After perfusion, liver samples were removed and washed in saline. Collected samples were flash-frozen immediately at −80°C for further assays (antioxidative effect; SOD, GPx, CAT, GSH and HO-1, lipid peroxidation; iNOS and NO, inflammation; TNF-α, a receptor; TLR4 and MyD88). All further assay procedures were carried out in accordance with the manufacturer's instruction.

2.7. Measurements of serum biochemical parameters

Serum samples were diluted for optimal reactions before being measured. The serum ALT and AST activities and ammonia level were measured by the optimal kits in accordance with the manufacture's instruction. The serum TNF-α protein expression was measured by ELISA.

2.8. Measurements of hepatic biochemical parameters.

Hepatic samples were diluted for optimal reactions before being measured. The enzymatic activities of SOD, GPx, CAT and GSH, and NO level were measured by colorimetric assays. The activity of hepatic iNOS, HO-1, Nf-κB, MyD88, and TLR4 were measured by an ELISA kit. All assay procedures were progressed according to the manufacturer's instructions.

2.9. Immunohistochemistry

Rat livers for immunohistochemistry were perfused in the same way as described previously. After being removed, liver samples were immersed for 2 weeks at room temperature. After immersing, liver samples were embedded in paraffin and were cut in 5-μm-thick cross sections using microtome. For staining of the expression of TLR4 and MyD88, TLR4 antibody (1:100) and MyD88 (1:100) antibodies were used; the secondary antibody was a Dako Real™ EnVision™ Detection System Rabbit/Mouse (1:200). After development with diaminobenzidine, sections were mounted on poly-lysine gelatinized glass slides and dehydrated through graded ethanol solutions before coverslipping.

Stained tissues were observed in Leica DMR 6000 microscope, and images were captured with a Leica DM 480 camera (Wetzlar, Germany). Images presented were photographed at 20 × 10 magnifications.

2.10. Hematoxylin and eosin and cresyl violet staining

Hematoxylin and eosin (H&E) staining was performed for detecting liver damage. Paraffin-embedded liver samples were cut in 5 μm thick using a microtome in the same way as

Table 1
Composition ratio of GBE and UGBE (%, w/w)

Ginsenoside	GBE	UGBE
Rb1	0.758 ± 0.179	0.072 ± 0.052#
Rb2	0.594 ± 0.114	0
Rd	1.534 ± 0.182	0.025 ± 0.007#
Re	11.169 ± 0.158	0.288 ± 0.037#
Rf	0.330 ± 0.115	0
Rg1	0.567 ± 0.013	0.033 ± 0.004*
Rg2	0.801 ± 0.215	2.278 ± 0.368*
20S-Rg3	0	0.432 ± 0.063*
20R-Rg3	0	0.400 ± 0.059*
Rg6	0.044 ± 0.026	0.445 ± 0.063*
Rh1	0.629 ± 0.095	1.350 ± 0.208*
Rh4	0	0.083 ± 0.011*
Rk1	0	0.2071 ± 0.030*
Rk3	0	0.039 ± 0.005*
F1	0.193 ± 0.149	0.035 ± 0.017
F4	0.191 ± 0.026	1.210 ± 0.137*

Ginsenoside Rb1, Rd, Re, Rg1, Rg2, RG3, RG6, Rh1, Rh4, Rk1, Rk3, F1, and F4 were detected in UGBE. Data represent mean ± S.E.M.
*$p < 0.05$ increased composition ratio of UGBE compared with same ginsenoside in GBE.
#$p < 0.05$ decreased composition ratio of UGBE compared to same ginsenosides in GBE.

described previously. Samples were then stained with H&E for detection of liver damage.

Stained tissues were observed with a Leica DMR 6000 microscope, and images were captured with a Leica DM 480 camera (Wetzlar, Germany). Low-magnification images presented were photographed at 20 × 10, and high-magnification images presented were photographed at 40 × 10.

2.11. Statistical analysis

The data are expressed as mean ± S.E.M. Statistical comparisons between each experimental group of all data were analyzed by the Student's *t*-test and one-way analysis of variance test. Differences were considered significant at error probabilities smaller than 0.05.

3. Results

3.1. HPLC analysis of UGBE

Table 1 shows the composition ratio of the GBE and UGBE analyzed by the HPLC systems [41]. The ginsenosides Rg2, Rg3, Rh1, Rh4, Rk1, Rk3, and F4 were significantly increased after 10-hr ultrasonication at 100C. Furthermore, ginsenosides Rg3 and Rk1 were newly produced in UGBE, which were not identified in GBE. HPLC chromatograms also proved these changes (Fig. 2) [42]. Fig. 3 shows the major component change between GBE and UGBE. Ginsenosides which were increased by ultrasonification had less polar residues than ginsenoside Re which was decreased by ultrasonification.

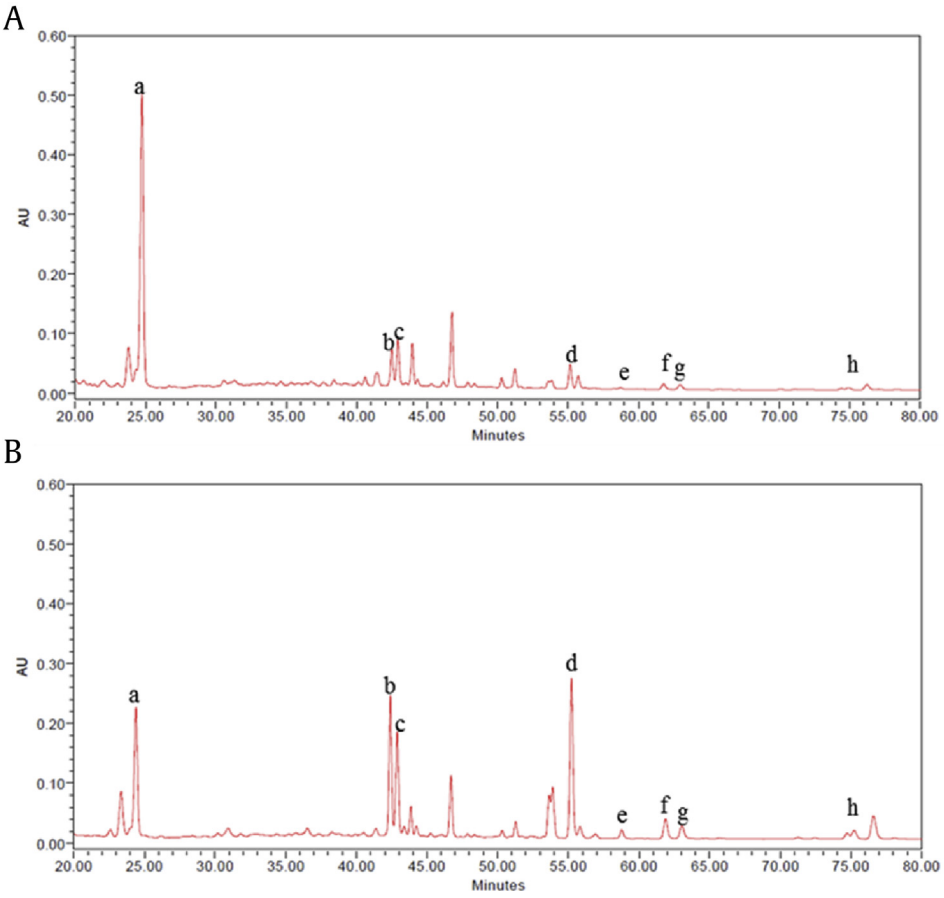

Fig. 2. High-performance liquid chromatography (HPLC) chromatograms of *Panax ginseng* berry extract and UGBE. (A) HPLC chromatogram of *P. ginseng* berry extract and (B) HPLC chromatogram of UGBE. The chromatograms were obtained using UV/Vis Waters 2478 Dual λ Absorbance Detector at 203 nm. a: ginsenoside Re, b: ginsenoside Rg2, c: ginsenoside Rh1, d: ginsenoside F4, e: ginsenoside Rk3 f: ginsenoside Rh4, g: ginsenoside Rg3, h: ginsenoside Rk1.

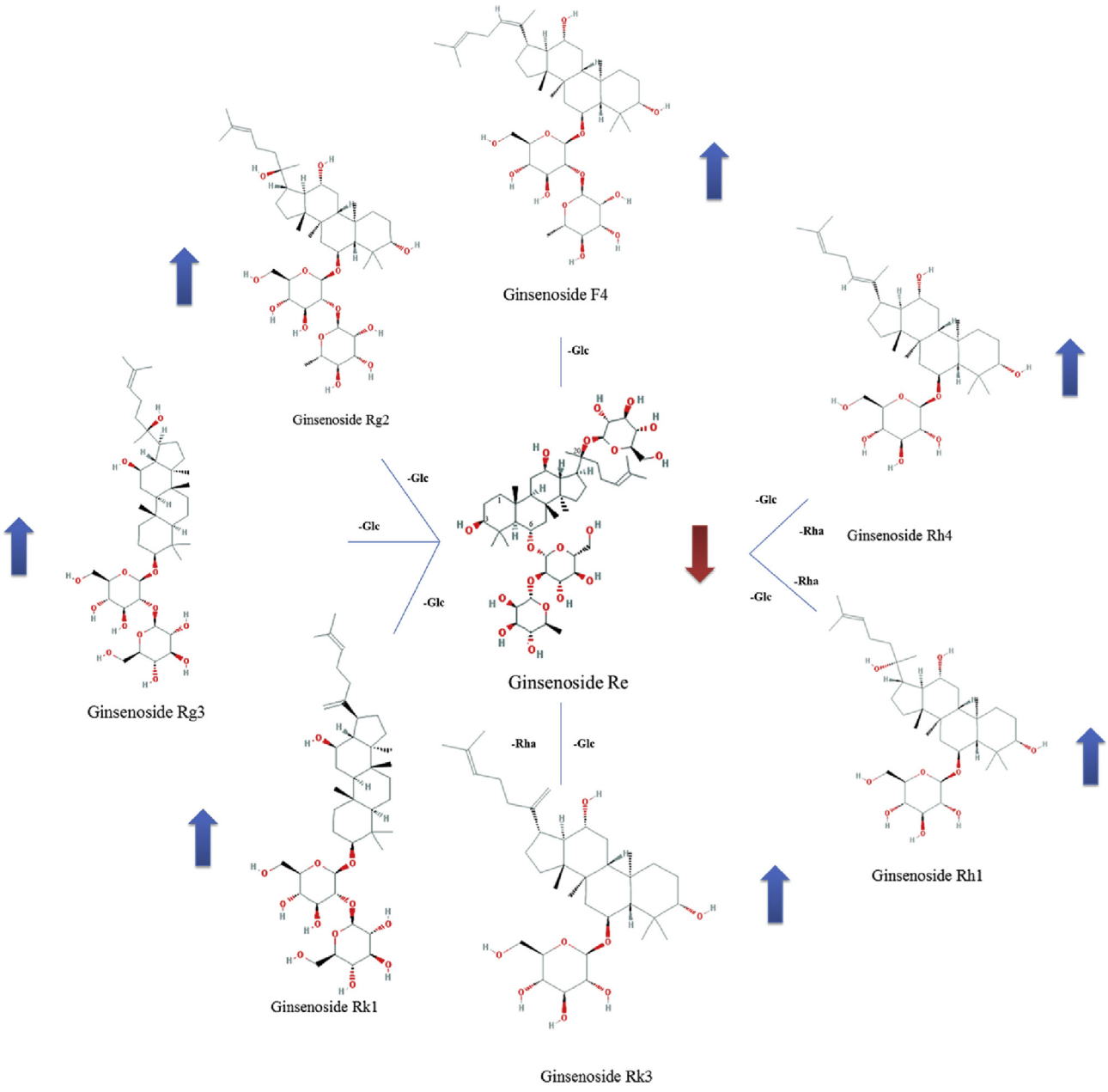

Fig. 3. Major component changes in *Panax ginseng* berry extract after ultrasonication. The ginsenoside Re was decreased by ultrasonication. Ginsenosides Rg3, Rg2, Rk1, F4, Rk3, Rh4, and Rh1 were increased by ultrasonication.

3.2. Effect of UGBE on liver dysfunction

AST and ALT are representative indicators of liver dysfunction. In this experiment, serum AST and ALT levels were measured (Table 2). The result shows that MBDL surgery significantly increased the activities of serum AST and ALT. However, administration of UGBE reduced the activities of serum AST and ALT in a dose-dependent manner. The treatment of low dosage of UGBE (100 mg/kg) showed better hepatoprotective effect than the treatment of silymarin (150 mg/kg). Also, serum ammonia level was measured as a result of liver dysfunction. The serum ammonia level in the experimental group showed similar tendencies to those of AST and ALT.

H&E staining results also supported the effect of UGBE on hepatotoxicity showing (Fig. 4). The control and sham group showed normal morphologies of liver. On the other hand, being compared with control and sham group, MBDL surgery group showed severe abnormal changes in hepatic lobules. In addition, the degeneration of hepatocyte, centrilobular necrosis, inflammatory cell infiltration, and inflammatory foci were frequently observed (Fig. 4C). GBE group also showed extensive histopathological changes such as hepatocytes degeneration, necrosis, and inflammatory cell infiltration (Fig. 4D). However, these histopathological changes were attenuated by the treatment of UGBE and silymarin. Especially, H&E staining results of UGBE2 and UGBE3 group showed normal morphology of hepatocyte (Figs. 4E–4H).

3.3. Effect of UGBE on oxidative stress in liver

Oxidative stress can accelerate liver dysfunction and hepatotoxicity. The activities of representative antioxidant enzymes such as SOD, GPx, and CAT were significantly decreased by MBDL surgery (Table 3). The treatment of GBE did not recover the function of

Table 2
Effect of UGBE on serum AST, ALT, and ammonia levels

	AST (IU/L)	ALT (IU/L)	Ammonia(μM)
Control	89.07 ± 10.13	50 ± 4.66	706.45 ± 82.63
Sham	91.37 ± 15.37	53.47 ± 8.67	753.91 ± 90.14
MBDL	173.51 ± 30.34***	122.46 ± 21.17***	1738.39 ± 133.71**
Sil	120.05 ± 10.62#	66.58 ± 10.87##	1137.42 ± 201.56##
GBE	158.54 ± 51.19	109.75 ± 20.16	1613.13 ± 88.82
UGBE1	115.19 ± 11.38#	65.64 ± 18.76##	1160.01 ± 118.26##
UGBE2	106.07 ± 9.91##	60.35 ± 8.98##	805.94 ± 92.13###
UGBE3	90.52 ± 13.43###	54.21 ± 7.76###	741.26 ± 103.57###

Control: control rats; Sham: Sham Operation control rats; MBDL: MBDL rats; Sil: MBDL rats Treated With silymarin (150 Mg/kg); GBE: MBDL rats Treated With GBE (150 Mg/kg); UGBE1: MBDL rats Treated With UGBE (100 Mg/kg); UGBE2: MBDL rats Treated With UGBE (250 Mg/kg); UGBE3: MBDL rats Treated With UGBE (500 Mg/kg).
Data are expressed as means ± S.E.M. (n = 9).
$^{***}p < 0.005$ Compared to control, $^{\#}p < 0.05$, $^{\#\#}p < 0.01$, $^{\#\#\#}p < 0.001$ compared with MBDL.

antioxidant enzymes, whereas the treatment of silymarin or UGBE did. Also, UGBE enhanced the protein expression of an inducible antioxidant enzymes against liver damage, HO-1, in dose-dependent manner. Even at low dosage (100 mg/kg), UGBE increased the antioxidant capacity of liver significantly. The treatment of GBE did not increase HO-1 levels against oxidative stress induced by MBDL surgery.

3.4. Effect of UGBE on iNOS and NO in liver

Free radicals also affect the pathogenesis of liver damage which is related to lipid peroxidation. The protein expression of iNOS and production of NO were investigated in liver (Fig. 5). In MBDL group, the protein expression of iNOS and the production of NO were significantly increased more than four times those of control group. However, the treatment of UGBE significantly decreased the protein expression of iNOS and production of NO, whereas the treatment of GBE did not.

3.5. Effect of UGBE on TLR4 signaling pathway

It is assumed that TLR4 signaling pathway might be involved in MBDL-induced liver dysfunction and hepatotoxicity. Based on this idea, the protein expression of TLR4 and its adaptable molecules, MyD88 were investigated (Figs. 6B and 6D). Our results showed that the treatment of UGBE significantly reduced MyD88-dependent TLR4 signaling pathway which increased by MBDL surgery. To further confirm the protein expression of TLR4 and MyD88, immunohistochemical analysis for TLR4 and MyD88 were conducted (Figs. 6A and 6C). The number of TLR4 and MyD88-positive cells in UGBE treatment group was decreased significantly compared with that in the MBDL group.

MyD88-dependent TLR4 signaling pathways activated the early phase of NF-κB, which produces inflammatory cytokines, including TNF-α. The expression of downstream signaling molecules of TLR4 signaling pathway, NF-κB, was reduced by UGBE treatment in a dose-dependent manner (Fig. 7A). Also, the protein expression of TNF-alpha was reduced by UGBE treatment (Fig. 7B). The treatment of GBE did not show the effect on upregulated TLR4 signaling pathway and overproduction of TNF-α induced by MBDL surgery.

4. Discussion

Owing to its various physiological effects, *P. ginseng* has gained huge interest for use in medicinal applications [43–47]. Several studies have shown the antidiabetic and antiobesity effects of ginsenoside Re, which is the major component of the *P. ginseng* berry [30,48,49]. However, another protective effect of ginsenosides on HE is still not clear. The aim of this study is to produce UGBE containing a high concentration of active prosapogenins and to evaluate the protective effect of UGBE on MBDL-induced rat HE model.

The composition ratio of UGBE and GBE were analyzed by HPLC. After ultrasonication process, ginsenoside Rb1, Rb2, Rd, Re, Rf, Rg1, Rg2, Rg3, Rg6, Rh1, Rh4, Rk1, Rk3, F1, and F4 were identified (Table 1). Among these ginsenosides, the composition ratio of most less polar ginsenosides, such as ginsenoside Rh1, Rh4, Rg2, Rg3, Rk1, Rk3, and F4, were largely increased from that produced during red ginseng's process of manufacture, whereas ginsenoside Re was decreased [50]. Several studies have investigated the effect of these compounds on the liver antioxidative, anti-inflammatory, and anti-carcinogenic effects of ginsenoside Rg2 and have been reported [51–54]. Ginsenoside Rk1 is known to have an anticancer effect in hepatocellular carcinoma cells [55,56]. Ginsenoside Rg3 has

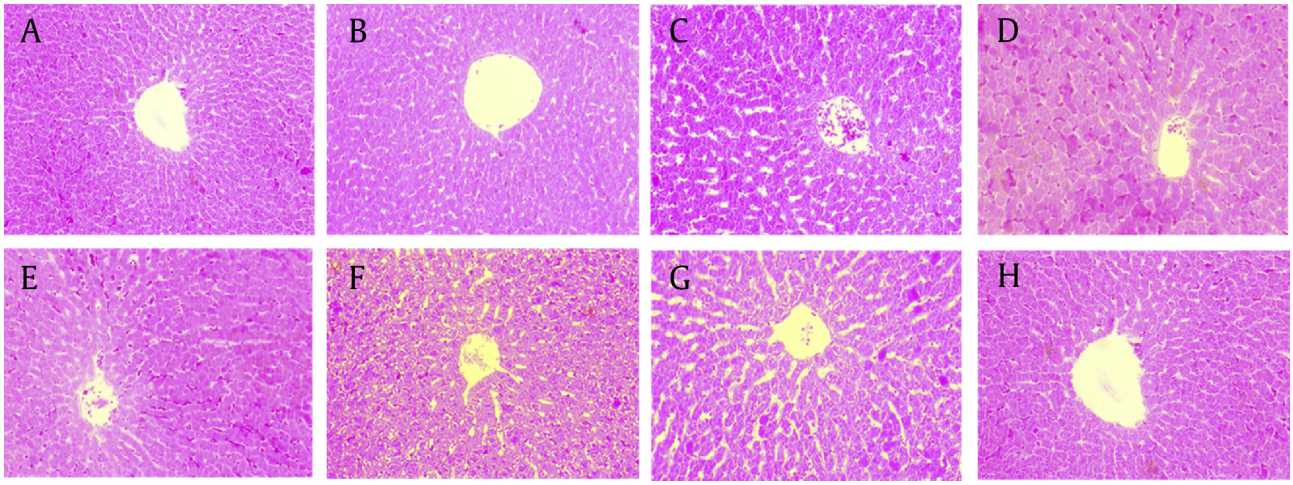

Fig. 4. Photomicrographs of liver section stained with hematoxylin and eosin. (A) Stained liver sections in control group, (B) sham-operation group, (C) mild bile duct ligation (MBDL) group, (D) silymarin treatment group, (E) *Panax ginseng* berry extract (GBE) treatment group, (F) UGBE1 treatment group, (G) UGBE2 treatment group, and (H) UGBE3 treatment group were observed and representative images of each section were captured at 20*10 magnifications. Control: control rats; Sham: sham operation control rats; MBDL: MBDL rats; Sil: MBDL rats treated with silymarin (150 mg/kg); GBE: MBDL rats treated with GBE (150 mg/kg); UGBE1: MBDL rats treated with UGBE (100 mg/kg); UGBE2: MBDL rats treated with UGBE (250 mg/kg); UGBE3: MBDL rats treated with UGBE (500 mg/kg).

Table 3
Effect of UGBE on oxidative stress

	GPx (U/mg)	SOD (U/mg)	CAT (U/mg)	HO-1 (ng/mg)
Control	23.26 ± 6.29	79.16 ± 10.23	12.26 ± 1.02	51.05 ± 7.44
Sham	25.14 ± 5.14	76.51 ± 7.55	11.84 ± 1.45	53.38 ± 8.87
MBDL	11.39 ± 3.17 ***	31.13 ± 5.17***	3.07 ± 0.96***	143.61 ± 20.05*
Sil	17.67 ± 5.83#	60.02 ± 12.31##	7.55 ± 2.16##	168.40 ± 14.12
GBE	13.05 ± 4.41	35.27 ± 18.94	3.66 ± 1.08	137.12 ± 18.53
UGBE1	18.05 ± 5.03##	61.48 ± 9.32##	7.95 ± 2.46##	184.48 ± 30.67##
UGBE2	20.94 ± 5.87###	70.05 ± 11.38##	10.67 ± 1.21###	216.63 ± 22.94###
UGBE3	22.48 ± 6.02###	77.18 ± 12.68###	12.34 ± 1.54###	262.68 ± 28.11###

Control: control rats; Sham: Sham Operation control rats; MBDL: MBDL rats; Sil: MBDL rats Treated With silymarin (150 Mg/kg); GBE: MBDL rats Treated With GBE (150 Mg/kg); UGBE1: MBDL rats Treated With UGBE (100 Mg/kg); UGBE2: MBDL rats Treated With UGBE (250 Mg/kg); UGBE3: MBDL rats Treated With UGBE (500 Mg/kg).
Data are expressed as means ± S.E.M. (n = 9).
$^{***}p < 0.005$ Compared to control, $^{\#}p < 0.05$, $^{\#\#}p < 0.01$, $^{\#\#\#}p < 0.001$ compared with MBDL.

antioxidative and hepatoprotective properties via the HO-1-related signaling pathway [57]. Ginsenoside Rh1 has been reported to exert an anti-inflammatory activity by inhibiting iNOS and cyclooxygenase-2 protein expression [58]. Ginsenoside F4 has shown an apoptosis-inducing effect that could be beneficial to organ protection [59,60].

With the ultrasonication processing, active ginsenosides were produced more than with typical red ginseng manufacturing. The primary ginsenosides of red ginseng are known to have an inhibitory effect on liver injury from a variety of mechanisms [61–63]. The ginsenosides Rg2, Rh1, and F4 are commonly produced in the complicated manufacturing process of red ginseng and exist in a

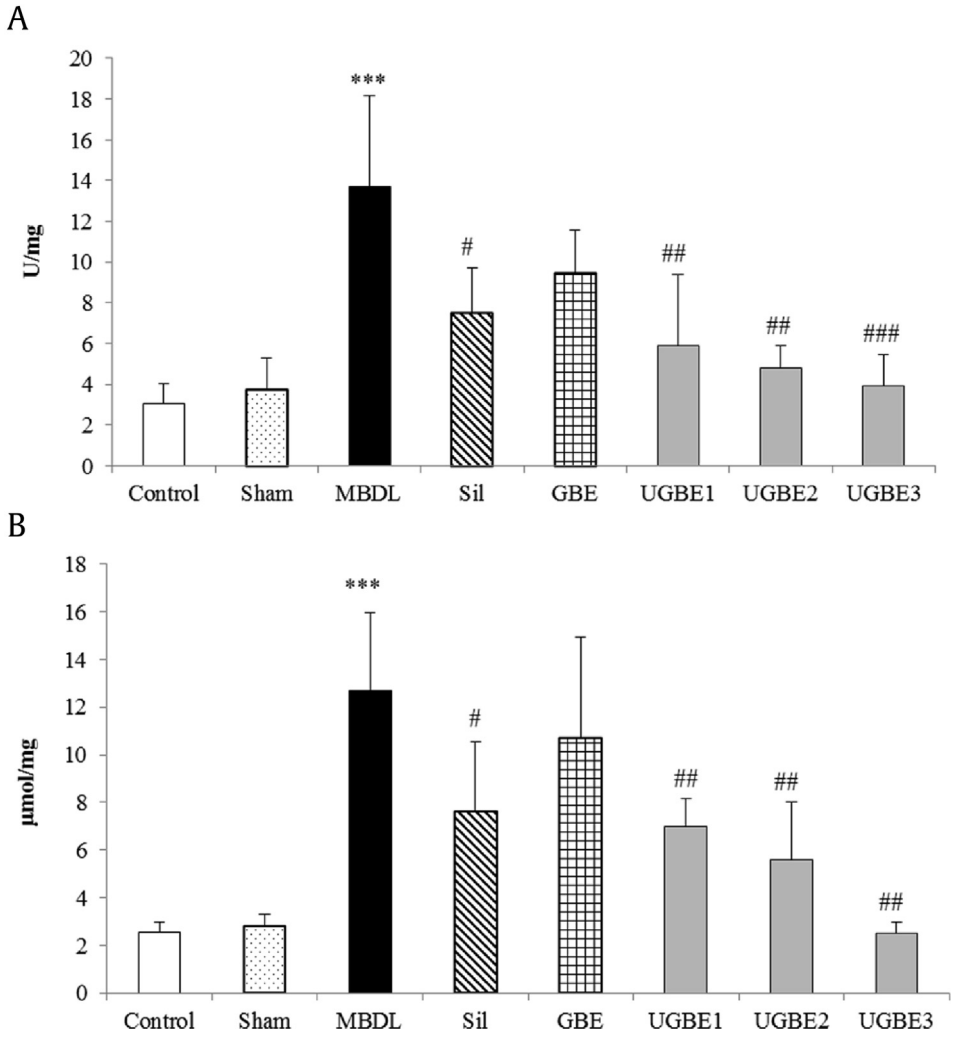

Fig. 5. Effect of UGBE on hepatic inducible nitric oxide synthase (iNOS) and NO levels. (A) Protein expression of iNOS in liver and (B) hepatic NO level. Control: control rats; Sham: sham operation control rats; MBDL: MBDL rats; Sil: MBDL rats treated with silymarin (150 mg/kg); GBE: MBDL rats treated with GBE (150 mg/kg); UGBE1: MBDL rats treated with UGBE (100 mg/kg); UGBE2: MBDL rats treated with UGBE (250 mg/kg); UGBE3: MBDL rats treated with UGBE (500 mg/kg). Data are expressed as means ± S.E.M. (n = 9). $^{***}p < 0.005$ compared to control, $^{\#}p < 0.05$, $^{\#\#}p < 0.01$, $^{\#\#\#}p < 0.001$ compared with MBDL.

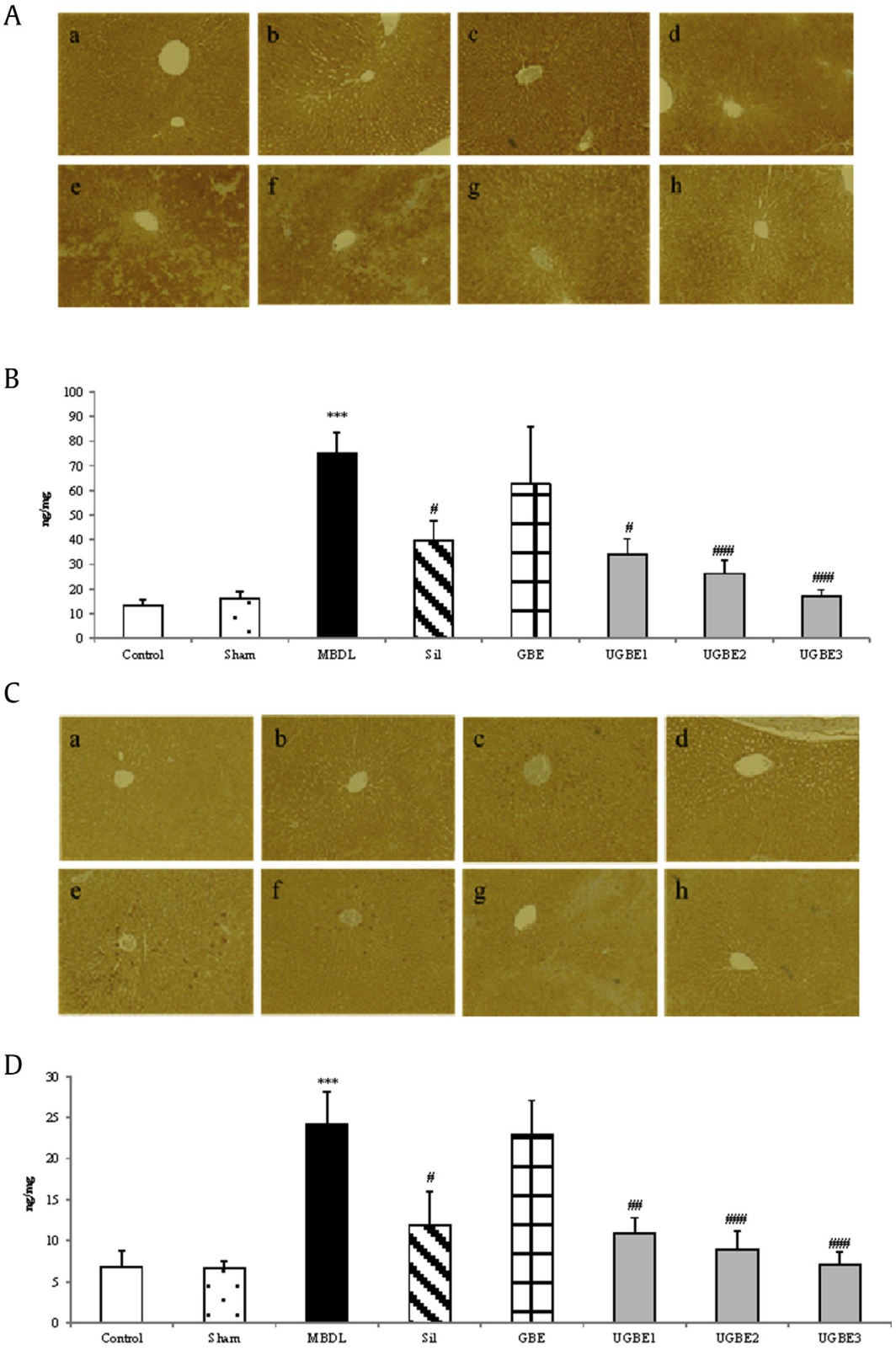

Fig. 6. Effect of UGBE on TLR4 signaling pathway. (B) and (D) are protein expression of TLR4 and MyD88 in liver, respectively. (A) and (C) are photomicrographs of TLR4 and MyD88 immunohistochemistry, respectively. Immunohistochemistry assays in stained liver sections were performed in liver and representative images were captured at 20*10 magnifications. Control: control rats; Sham: sham operation control rats; MBDL: MBDL rats; Sil: MBDL rats treated with silymarin (150 mg/kg); GBE: MBDL rats treated with GBE (150 mg/kg); UGBE1: MBDL rats treated with UGBE (100 mg/kg); UGBE2: MBDL rats treated with UGBE (250 mg/kg); UGBE3: MBDL rats treated with UGBE (500 mg/kg). a: control group, b: sham-operation group, c: MBDL group, d: silymarin treatment group, e: GBE treatment group, f: UGBE1 treatment group, g: UGBE2 treatment group and h: UGBE3 treatment group. Data are expressed as means ± S.E.M. (n = 9). $^{***}p < 0.005$ compared to control, $^{\#}p < 0.05$, $^{\#\#}p < 0.01$, $^{\#\#\#}p < 0.001$ compared with MBDL.

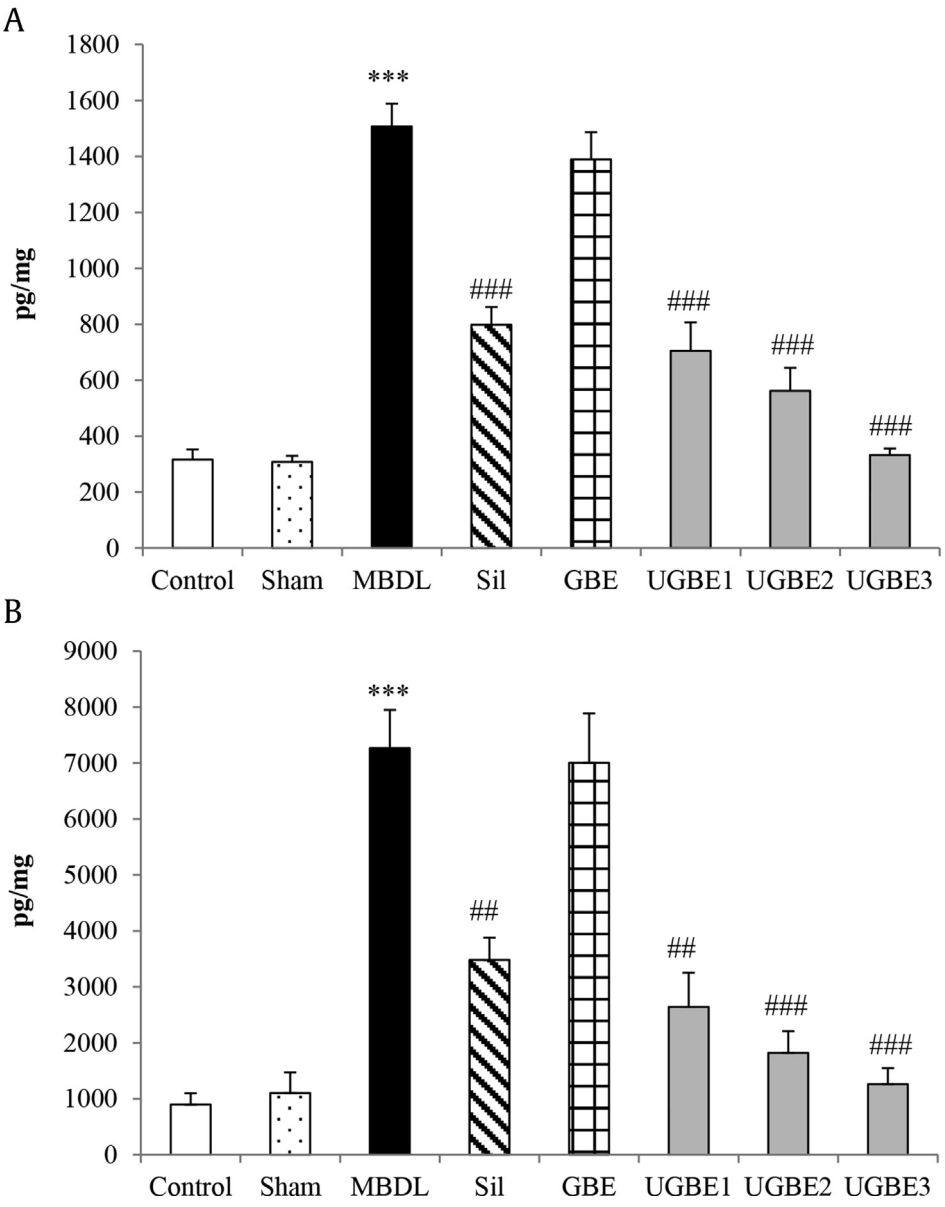

Fig. 7. Effect of UGBE on nuclear factor–kappa B (NF-κB) and tumor necrosis factor-alpha (TNF-α). (A) Protein expression of total (p65) NF-κB. (B) Protein expression of TNF-α in liver. Control: control rats; Sham: sham operation control rats; MBDL: MBDL rats; Sil: MBDL rats treated with silymarin (150 mg/kg); GBE: MBDL rats treated with GBE (150 mg/kg); UGBE1: MBDL rats treated with UGBE (100 mg/kg); UGBE2: MBDL rats treated with UGBE (250 mg/kg); UGBE3: MBDL rats treated with UGBE (500 mg/kg). Data are expressed as means ± S.E.M. (n = 9). $^{***}p < 0.005$ compared to control, $^{\#}p < 0.05$, $^{\#\#}p < 0.01$, $^{\#\#\#}p < 0.001$ compared with MBDL.

small amount in *P. ginseng* berry [50,64]. The effect of the UGBE on liver is still in a veil. However, the potential of this ginsenoside on liver is expected to be useful.

Biliary obstruction or biliary drainage is a common pathophysiology of HE patients [65]. Once bile duct is ligated, the liver cannot excrete bile acid that could be strong toxicant itself in liver, which causes cholestatic liver disease and dysfunction [66]. Liver dysfunction often leads to overproduction of ammonia in liver [67,68]. BDL surgery induces liver fibrosis and inflammation directly and definitely by an undercurrent of bile acid in liver, whereas PVL or PCA surgery remains a controversy in the induction of HE condition [69,70]. The difference might be due to the uncertainty of ischemic condition and the way biochemical parameters are measured [71]. In this experiment, MBDL model was used instead of BDL surgery to induce liver fibrosis in rats. MBDL model has shown a longer survival than BDL rats, i.e., more than 3 months, allowing researchers to study the long-term effect on liver damage [40]. Although several studies reported the difference between BDL and MBDL models in the pattern of liver dysfunction, our MBDL induced liver fibrosis sufficiently without cirrhosis. The main differences are only the survival rate and rapidity of inflammatory liver injury [40].

In the present study, MBDL surgery significantly increased the levels of the representative indicator of liver dysfunction (serum ALT, AST, and ammonia) by MBDL surgery in rats. However, the long-term administration of UGBE recovered the liver function and serum ammonia level, dose-dependently (Table 2). H&E staining also supports these results (Fig. 4). Meanwhile, GBE did not affect the liver dysfunction induced by BDL surgery. The liver dysfunction by biliary obstruction is characterized by increased serum ammonia levels [72]. Ammonia level in serum is closely correlated with the severity of inflammatory liver injury [73]. At

physiological pH, the majority (98%) of ammonia is found in ionic form (NH_4^+) with ~2% arising in gas form (NH_3). Both forms are capable of crossing cellular membranes. NH_3 mainly pass through the cellular membrane through diffusion. Meanwhile, NH_4^+ cross the cellular membrane via K^+ channels and cotransporters since NH_4^+ has very similar ionic properties (ionic radius and diffusion coefficient) to K^+. The differences between GBE and UGBE on liver dysfunction may be due to the composition ratio of ginsenosides. In this study, we confirmed that the UGBE decreased serum ammonia level and restored liver function significantly in rat MBDL model. These result suggested that the UGBE has huge potential to be developed as a cure for HE.

In the liver dysfunction, oxidative stress plays a crucial role in contributing to the initiation and progression of hepatic failure, especially in inflammatory liver disorders [74–76]. The enzyme-dependent antioxidative system plays important roles in reactive oxygen species (ROS)-induced liver damage [77]. The BDL surgery resulted in the imbalance of ROS production and the impairment of the antioxidant capacity of the liver [78]. Overproduction of ROS inactivates antioxidative enzymes such as SOD, CAT, and GPx in the BDL-induced inflammatory liver injury model in rats [79]. Recovery of these enzymes suggests that treatment of UGBE recovered liver dysfunction and reduced oxidative stress-induced by MBDL surgery effectively. Furthermore, HO-1 plays an important role in cyto-protection by decreasing the leukocytic response and ameliorating BD-induced liver damage [80]. HO-1 is an enzyme that catalyzes the degradation of heme into bilirubin, carbon monoxide, and free iron [81]. HO-1 expression increased dose-dependently according to UGBE treatment (Table 3). These results indicate that UGBE enhanced the hepatoprotective effect by increasing the HO-1 protein expression and is likely mediated by ginsenoside Rg2 [57]. The findings of the present study reveal that administration of UGBE protects antioxidative enzymes from oxidative damage (Table 3). Although it has not been identified that UGBE directly scavenges ROS, there is a strong likelihood that that UGBE increased the antioxidant capacity and ameliorated oxidative stress against MBDL-induced hepatotoxicity.

The expression of iNOS in hepatic ischemia-reperfusion injury aggravates the pathogenesis of chronic liver injury by increasing lipid peroxidation in hepatic macrophage [82,83]. NO produced by iNOS dramatically reacts with ROS to form peroxynitrite (ONOOK) which is a toxic agent for liver [84]. In the present study, UGBE ameliorated MBDL-induced hepatotoxicity. The oral administration of UGBE significantly suppressed the protein expression of iNOS and the production of NO, whereas GBE was ineffective (Fig. 5). It is assumed that the hepatoprotective effect of UGBE is related not only with hepatocyte but also with macrophage in the liver.

Several studies have reported the correlation between BDL-induced liver injury and TLR4 through bacterial translocation [85–87]. Activation of TLR4 can signal through NF-κB nuclear location which results in the production of inflammatory cytokines [88]. There are two types of TLR4 signaling pathway, including MyD88-dependent and MyD88-independent (TRIF-related adaptor molecule; TRAM) signaling pathways [89]. MyD88 is an adaptor molecule that signals TLR4 signaling predominantly [90]. In our MBDL model, MyD88 signaled TLR4 signaling pathway, whereas MyD88-independent signaling pathway did not (data not shown). The UGBE treatment reduced the protein expression of TLR4 and MyD88 (Fig. 6). The NF-κB ELISA assay showed the same result with TLR4 and MyD88 (Fig. 6A). These results indicate that the protective effect of UGBE on BDL induced liver injury relies on TLR4 receptor signaling pathway.

TNF-α, representative proinflammatory cytokines-induced by TLR4 signaling pathway, is an important proinflammatory cytokine that triggers liver damage in the BDL-induced liver fibrosis model [91]. TNF-α also plays an important role in hepatotoxicity related to free-radical-mediated apoptosis [92]. Hepatic TNF-α levels were also reduced with UGBE treatment in a dose-dependent manner (Fig. 7B).

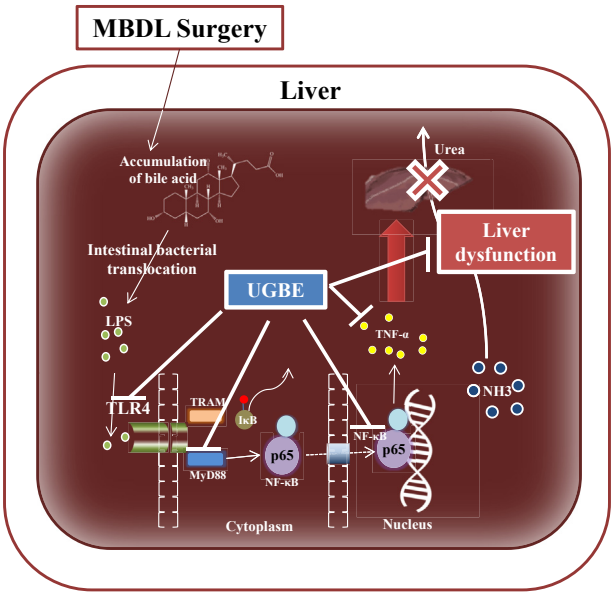

Fig. 8. The graphical summary. The mild bile duct ligation (MBDL) surgery is induced severe hepatotoxicity which leads to liver inflammation in rats. Also, the serum ammonia level was increased by MBDL surgery. However, the liver dysfunction of MBDL surgery operated rats was attenuated by UGBE treatment via myeloid differentiation factor 88-dependent toll-like receptor 4 signaling pathways.

Based on the results of the present study, it can be summarized that MBDL-induced liver damage was ameliorated by oral administration of UGBE (Fig. 8). Oral administration of UGBE reduced hepatotoxicity in the liver, which induced by MBDL surgery. Also, the serum ammonia level was reduced by administration of UGBE. This protective effect is mediated by suppression of TLR4 protein expression in liver. Consequently, the UGBE showed great protective effect on MBDL-induced liver fibrosis and inflammatory liver injury model in rats and a potential to be developed as a new remedy for liver fibrosis.

Conflicts of interest

All authors have no conflicts of interest to declare.

Source of funding

The authors declare no source of funding.

Others

Experiments were done by Y.N. in pharmacology laboratory in Chung-Ang University. The extract used in this article is kindly provided by S.K.K.. U.D.S. organized all procedure related to this article. This manuscript was not presented in any poster meeting as well as elsewhere.

Acknowledgments

This research was supported by High Value-added Food Technology Development Program, Ministry of Agriculture, Food and Rural Affairs (113021-03).

References

[1] Baiocchini A, Montaldo C, Conigliaro A, Grimaldi A, Correani V, Mura F, Ciccosanti F, Rotiroti N, Brenna A, Montalbano M, et al. Extracellular matrix molecular remodeling in human liver fibrosis evolution. PloS One 2016;11: e0151736.

[2] Lin X, Zhang S, Huang Q, Wei L, Zheng L, Chen Z, Jiao Y, Huang J, Fu S, Huang R. Protective effect of fufang-liu-Yue-qing, a traditional Chinese herbal formula, on ccl4 induced liver fibrosis in rats. J Ethnopharmacol 2012;142:548–56.

[3] Zelber-Sagi S, Shoham D, Zvibel I, Abu-Abeid S, Shibolet O, Fishman S. Predictors for advanced fibrosis in morbidly obese non-alcoholic fatty liver patients. World J Hepatol 2017;9:91–8.

[4] Weber LW, Boll M, Stampfl A. Hepatotoxicity and mechanism of action of haloalkanes: carbon tetrachloride as a toxicological model. Crit Rev Toxicol 2003;33:105–36.

[5] Rodrigo R, Cauli O, Gomez-Pinedo U, Agusti A, Hernandez-Rabaza V, Garcia-Verdugo JM, Felipo V. Hyperammonemia induces neuroinflammation that contributes to cognitive impairment in rats with hepatic encephalopathy. Gastroenterology 2010;139:675–84.

[6] Nusrat S, Khan MS, Fazili J, Madhoun MF. Cirrhosis and its complications: evidence based treatment. World J Gastroenterol: WJG 2014;20:5442–60.

[7] Bohte AE, van Dussen L, Akkerman EM, Nederveen AJ, Sinkus R, Jansen PL, Stoker J, Hollak CE. Liver fibrosis in type i gaucher disease: magnetic resonance imaging, transient elastography and parameters of iron storage. PloS One 2013;8. e57507.

[8] Wijdicks EF. Hepatic encephalopathy. New Engl J Med 2016;375:1660–70.

[9] Weber Jr FL. Lactulose and combination therapy of hepatic encephalopathy: the role of the intestinal microflora. Dig Dis 1996;14(Suppl 1):53–63.

[10] Oku T, Nakamura S. Estimation of intestinal trehalase activity from a laxative threshold of trehalose and lactulose on healthy female subjects. Eur J Clin Nutr 2000;54:783–8.

[11] He F, Dai S, Xiao Z, Wang L, Yue Z, Zhao H, Zhao M, Lin Q, Dong X, Liu F. Pathological predictors of shunt stenosis and hepatic encephalopathy after transjugular intrahepatic portosystemic shunt. BioMed Res Int 2016;2016. 3681731.

[12] Jonsson JR, Barrie HD, O'Rourke P, Clouston AD, Powell EE. Obesity and steatosis influence serum and hepatic inflammatory markers in chronic hepatitis c. Hepatology 2008;48:80–7.

[13] Carpino G, Nobili V, Renzi A, De Stefanis C, Stronati L, Franchitto A, Alisi A, Onori P, De Vito R, Alpini G, et al. Macrophage activation in pediatric nonalcoholic fatty liver disease (nafld) correlates with hepatic progenitor cell response via wnt3a pathway. PloS One 2016;11. e0157246.

[14] Zhao HW, Zhang ZF, Chai X, Li GQ, Cui HR, Wang HB, Meng YK, Liu HM, Wang JB, Li RS, et al. Oxymatrine attenuates ccl4-induced hepatic fibrosis via modulation of tlr4-dependent inflammatory and tgf-beta1 signaling pathways. Int Immunopharmacol 2016;36:249–55.

[15] Calvo-Rodriguez M, de la Fuente C, Garcia-Durillo M, Garcia-Rodriguez C, Villalobos C, Nunez L. Aging and amyloid beta oligomers enhance tlr4 expression, lps-induced ca2+ responses, and neuron cell death in cultured rat hippocampal neurons. J Neuroinflammation 2017;14:24.

[16] Shimizu M, Ogura K, Mizoguchi I, Chiba Y, Higuchi K, Ohtsuka H, Mizuguchi J, Yoshimoto T. Il-27 promotes nitric oxide production induced by lps through stat1, nf-kappab and mapks. Immunobiology 2013;218:628–34.

[17] Song Y, Dou H, Gong W, Liu X, Yu Z, Li E, Tan R, Hou Y. Bis-n-norgliovictin, a small-molecule compound from marine fungus, inhibits lps-induced inflammation in macrophages and improves survival in sepsis. Eur J Pharmacol 2013;705:49–60.

[18] Mancek-Keber M, Frank-Bertoncelj M, Hafner-Bratkovic I, Smole A, Zorko M, Pirher N, Hayer S, Kralj-Iglic V, Rozman B, Ilc N, et al. Toll-like receptor 4 senses oxidative stress mediated by the oxidation of phospholipids in extracellular vesicles. Sci Signal 2015;8:ra60.

[19] Oya S, Yokoyama Y, Kokuryo T, Uno M, Yamauchi K, Nagino M. Inhibition of toll-like receptor 4 suppresses liver injury induced by biliary obstruction and subsequent intraportal lipopolysaccharide injection. Am J Physiol Gastrointest Liver Physiol 2014;306:G244–52.

[20] Cubero FJ, Zoubek ME, Hu W, Peng J, Zhao G, Nevzorova YA, Al Masaoudi M, Bechmann LP, Boekschoten MV, Muller M, et al. Combined activities of jnk1 and jnk2 in hepatocytes protect against toxic liver injury. Gastroenterology 2016;150:968–81.

[21] Maruoka R, Aoki N, Kido M, Iwamoto S, Nishiura H, Ikeda A, Chiba T, Watanabe N. Splenectomy prolongs the effects of corticosteroids in mouse models of autoimmune hepatitis. Gastroenterology 2013;145:209–20. e209.

[22] Perepelyuk M, Terajima M, Wang AY, Georges PC, Janmey PA, Yamauchi M, Wells RG. Hepatic stellate cells and portal fibroblasts are the major cellular sources of collagens and lysyl oxidases in normal liver and early after injury. Am J Physiol Gastrointest Liver Physiol 2013;304:G605–14.

[23] Tag CG, Weiskirchen S, Hittatiya K, Tacke F, Tolba RH, Weiskirchen R. Induction of experimental obstructive cholestasis in mice. Lab Anim 2015;49:70–80.

[24] Redwan AA. Complex post-cholecystectomy biliary injuries: management with 10 years' experience in a major referral center. J Laparoendosc Adv Surg Tech A Part A 2012;22:539–49.

[25] Eken H, Ozturk H, Buyukbayram H. Dose-related effects of dexamethasone on liver damage due to bile duct ligation in rats. World J Gastroenterol: WJG 2006;12:5379–83.

[26] Yun TK. Panax ginseng–a non-organ-specific cancer preventive? Lancet Oncol 2001;2:49–55.

[27] Yang SO, Park HR, Sohn ES, Lee SW, Kim HD, Kim YC, Kim KH, Na SW, Choi HK, Arasu MV, et al. Classification of ginseng berry (panax ginseng c.A. Meyer) extract using 1h nmr spectroscopy and its inhibition of lipid accumulation in 3 t3-l1 cells. BMC Complement Altern Med 2014;14:455.

[28] Choi KT. Botanical characteristics, pharmacological effects and medicinal components of Korean panax ginseng c a meyer. Acta Pharmacol Sin 2008;29: 1109–18.

[29] Zhao H, Li Q, Pei X, Zhang Z, Yang R, Wang J, Li Y. Long-term ginsenoside administration prevents memory impairment in aged c57bl/6j mice by up-regulating the synaptic plasticity-related proteins in hippocampus. Behav Brain Res 2009;201:311–7.

[30] Quan HY, Yuan HD, Jung MS, Ko SK, Park YG, Chung SH. Ginsenoside re lowers blood glucose and lipid levels via activation of amp-activated protein kinase in hepg2 cells and high-fat diet fed mice. Int J Mol Med 2012;29:73–80.

[31] Deng HL, Zhang JT. Anti-lipid peroxilative effect of ginsenoside rb1 and rg1. Chin Med J 1991;104:395–8.

[32] Ma L, Liu H, Xie Z, Yang S, Xu W, Hou J, Yu B. Ginsenoside rb3 protects cardiomyocytes against ischemia-reperfusion injury via the inhibition of jnk-mediated nf-kappab pathway: a mouse cardiomyocyte model. PloS One 2014;9. e103628.

[33] Attele AS, Wu JA, Yuan CS. Ginseng pharmacology: multiple constituents and multiple actions. Biochem Pharmacol 1999;58:1685–93.

[34] Kim CK, Cho DH, Lee KS, Lee DK, Park CW, Kim WG, Lee SJ, Ha KS, Goo Taeg O, Kwon YG, et al. Ginseng berry extract prevents atherogenesis via anti-inflammatory action by upregulating phase ii gene expression. *Evidence-based complementary and alternative medicine*. eCAM 2012:2012. 490301.

[35] Lu JM, Yao Q, Chen C. Ginseng compounds: an update on their molecular mechanisms and medical applications. Curr Vasc Pharmacol 2009;7:293–302.

[36] Kim YK, Yoo DS, Xu H, Park NI, Kim HH, Choi JE, Park SU. Ginsenoside content of berries and roots of three typical Korean ginseng (panax ginseng) cultivars. Nat Prod Commun 2009;4:903–6.

[37] Jayakodi M, Lee SC, Lee YS, Park HS, Kim NH, Jang W, Lee HO, Joh HJ, Yang TJ. Comprehensive analysis of panax ginseng root transcriptomes. BMC Plant Biol 2015;15:138.

[38] Yang W, Qiao X, Li K, Fan J, Bo T, Guo DA, Ye M. Identification and differentiation of panax ginseng, panax quinquefolium, and panax notoginseng by monitoring multiple diagnostic chemical markers. Acta Pharm Sin B 2016;6: 568–75.

[39] Lee SJ, Kim Y, Kim MG. Changes in the ginsenoside content during the fermentation process using microbial strains. J Ginseng Res 2015;39:392–7.

[40] Gimenez-Garzo C, Salhi D, Urios A, Ruiz-Sauri A, Carda C, Montoliu C, Felipo V. Rats with mild bile duct ligation show hepatic encephalopathy with cognitive and motor impairment in the absence of cirrhosis: effects of alcohol ingestion. Neurochem Res 2015;40:230–40.

[41] Jung H, Bae J, Ko SK, Sohn UD. Ultrasonication processed panax ginseng berry extract induces apoptosis through an intrinsic apoptosis pathway in hepg2 cells. Arch Pharm Res 2016;39:855–62.

[42] Nam Y, Bae J, Jeong JH, Ko SK, Sohn UD. Protective effect of ultrasonication-processed ginseng berry extract on the d-galactosamine/lipopolysaccharide-induced liver injury model in rats. J Ginseng Res 2018;42:540–8.

[43] Choi JS, Chun KS, Kundu J, Kundu JK. Biochemical basis of cancer chemoprevention and/or chemotherapy with ginsenosides (review). Int J Mol Med 2013;32:1227–38.

[44] Kang JH, Song KH, Woo JK, Park MH, Rhee MH, Choi C, Oh SH. Ginsenoside rp1 from panax ginseng exhibits anti-cancer activity by down-regulation of the igf-1r/akt pathway in breast cancer cells. Plant Foods Hum Nutr 2011;66: 298–305.

[45] Wang Y, Kan H, Yin Y, Wu W, Hu W, Wang M, Li W. Protective effects of ginsenoside rg1 on chronic restraint stress induced learning and memory impairments in male mice. Pharmacol Biochem Behav 2014;120:73–81.

[46] Kimura Y, Sumiyoshi M, Sakanaka M. Effects of ginsenoside rb(1) on skin changes. J Biomed Biotechnol 2012:2012. 946242.

[47] Paul S, Shin HS, Kang SC. Inhibition of inflammations and macrophage activation by ginsenoside-re isolated from Korean ginseng (panax ginseng c.A. Meyer). Food Chem Toxicol: An Int J Publ Br Ind Biol Res Assoc 2012;50:1354–61.

[48] Han DH, Kim SH, Higashida K, Jung SR, Polonsky KS, Klein S, Holloszy JO. Ginsenoside re rapidly reverses insulin resistance in muscles of high-fat diet fed rats. Metabol: Clin Ex 2012;61:1615–21.

[49] Liu YW, Zhu X, Li W, Lu Q, Wang JY, Wei YQ, Yin XX. Ginsenoside re attenuates diabetes-associated cognitive deficits in rats. Pharmacol Biochem Behav 2012;101:93–8.

[50] Lee SA, Jo HK, Im BO, Kim S, Whang WK, Ko SK. Changes in the contents of prosapogenin in the red ginseng (panax ginseng) depending on steaming batches. J Ginseng Res 2012;36:102–6.

[51] Jang HJ, Han IH, Kim YJ, Yamabe N, Lee D, Hwang GS, Oh M, Choi KC, Kim SN, Ham J, et al. Anticarcinogenic effects of products of heat-processed ginsenoside re, a major constituent of ginseng berry, on human gastric cancer cells. J Agric Food Chem 2014;62:2830–6.

[52] Fu W, Sui D, Yu X, Gou D, Zhou Y, Xu H. Protective effects of ginsenoside rg2 against h2o2-induced injury and apoptosis in h9c2 cells. Int J Clin Exp Med 2015;8:19938–47.

[53] Jung JS, Lee SY, Kim DH, Kim HS. Protopanaxatriol ginsenoside rh1 upregulates phase ii antioxidant enzyme gene expression in rat primary astrocytes: involvement of map kinases and nrf2/are signaling. Biomol Ther 2016;24:33–9.
[54] Lee SY, Jeong JJ, Eun SH, Kim DH. Anti-inflammatory effects of ginsenoside rg1 and its metabolites ginsenoside rh1 and 20(s)-protopanaxatriol in mice with tnbs-induced colitis. Eur J Pharmacol 2015;762:333–43.
[55] Kim YJ, Kwon HC, Ko H, Park JH, Kim HY, Yoo JH, Yang HO. Anti-tumor activity of the ginsenoside rk1 in human hepatocellular carcinoma cells through inhibition of telomerase activity and induction of apoptosis. Biol Pharmaceut Bull 2008;31:826–30.
[56] Ko H, Kim YJ, Park JS, Park JH, Yang HO. Autophagy inhibition enhances apoptosis induced by ginsenoside rk1 in hepatocellular carcinoma cells. Biosci Biotechnol Biochem 2009;73:2183–9.
[57] Lee CK, Park KK, Chung AS, Chung WY. Ginsenoside rg3 enhances the chemosensitivity of tumors to cisplatin by reducing the basal level of nuclear factor erythroid 2-related factor 2-mediated heme oxygenase-1/nad(p)h quinone oxidoreductase-1 and prevents normal tissue damage by scavenging cisplatin-induced intracellular reactive oxygen species. Food Chem Toxicol: Int JournalPubl Br Ind Biol Res Assoc 2012;50:2565–74.
[58] Park EK, Choo MK, Han MJ, Kim DH. Ginsenoside rh1 possesses antiallergic and anti-inflammatory activities. Int Arch Allergy Immunol 2004;133:113–20.
[59] Chen B, Shen YP, Zhang DF, Cheng J, Jia XB. The apoptosis-inducing effect of ginsenoside f4 from steamed notoginseng on human lymphocytoma jk cells. Nat Prod Res 2013;27:2351–4.
[60] Guicciardi ME, Gores GJ. Apoptosis: a mechanism of acute and chronic liver injury. Gut 2005;54:1024–33.
[61] Gum SI, Cho MK. Korean red ginseng extract prevents apap-induced hepatotoxicity through metabolic enzyme regulation: the role of ginsenoside rg3, a protopanaxadiol. Liver Int: Official J Int Assoc Study Liver 2013;33:1071–84.
[62] Igami K, Shimojo Y, Ito H, Miyazaki T, Kashiwada Y. Hepatoprotective effect of fermented ginseng and its major constituent compound k in a rat model of paracetamol (acetaminophen)-induced liver injury. J Pharm Pharmacol 2014.
[63] Park HM, Kim SJ, Kim JS, Kang HS. Reactive oxygen species mediated ginsenoside rg3- and rh2-induced apoptosis in hepatoma cells through mitochondrial signaling pathways. Food Chem Toxicol: Int J Publ Br Ind Biol Res Assoc 2012;50:2736–41.
[64] Kim MH, Lee YC, Choi SY, Cho CW, Rho J, Lee KW. The changes of ginsenoside patterns in red ginseng processed by organic acid impregnation pretreatment. J Ginseng Res 2011;35:497–503.
[65] Ishizawa T, Hasegawa K, Sano K, Imamura H, Kokudo N, Makuuchi M. Selective versus total biliary drainage for obstructive jaundice caused by a hepatobiliary malignancy. Am J Surg 2007;193:149–54.
[66] Luo B, Abrams GA, Fallon MB. Endothelin-1 in the rat bile duct ligation model of hepatopulmonary syndrome: correlation with pulmonary dysfunction. J Hepatol 1998;29:571–8.
[67] Bemeur C, Butterworth RF. Liver-brain proinflammatory signalling in acute liver failure: role in the pathogenesis of hepatic encephalopathy and brain edema. Metab Brain Dis 2013;28:145–50.
[68] Monzani PS, Moraes G. Urea cycle enzymes through the development of pacu (piaractus mesopotamicus): the role of ornithine carbamoyl transferase. Fish Physiol Biochem 2008;34:139–49.
[69] Bruck J, Gorg B, Bidmon HJ, Zemtsova I, Qvartskhava N, Keitel V, Kircheis G, Haussinger D. Locomotor impairment and cerebrocortical oxidative stress in portal vein ligated rats in vivo. J Hepatol 2011;54:251–7.
[70] Cauli O, Llansola M, Erceg S, Felipo V. Hypolocomotion in rats with chronic liver failure is due to increased glutamate and activation of metabotropic glutamate receptors in substantia nigra. J Hepatol 2006;45:654–61.
[71] Leke R, de Oliveira DL, Mussulini BH, Pereira MS, Kazlauckas V, Mazzini G, Hartmann CR, Silveira TR, Simonsen M, Bak LK, et al. Impairment of the organization of locomotor and exploratory behaviors in bile duct-ligated rats. PloS One 2012;7. e36322.
[72] Chang CC, Chen YC, Huang HC, Lee FY, Chang FY, Lin HC, Chan CY, Wang SS, Lee SD. Methimazole alleviates hepatic encephalopathy in bile-duct ligated cirrhotic rats. J Chin Med Assoc: JCMA 2006;69:563–8.
[73] Wang V, Saab S. Ammonia levels and the severity of hepatic encephalopathy. Am J Med 2003;114:237–8.
[74] Lu J, Chen YP, Wan R, Guo CY, Wang XP. Protective effects of ulinastatin on acute liver failure induced by lipopolysaccharide/d-galactosamine. Dig Dis Sci 2012;57:399–404.
[75] Singal AK, Jampana SC, Weinman SA. Antioxidants as therapeutic agents for liver disease. Liver Int: Off J Int Assoc Study Liver 2011;31:1432–48.
[76] Esrefoglu M. Oxidative stress and benefits of antioxidant agents in acute and chronic hepatitis. Hepat Mon 2012;12:160–7.
[77] Ai G, Liu Q, Hua W, Huang Z, Wang D. Hepatoprotective evaluation of the total flavonoids extracted from flowers of abelmoschus manihot (l.) medic: in vitro and in vivo studies. J Ethnopharmacol 2013;146:794–802.
[78] Ayvaz S, Kanter M, Aksu B, Sahin SH, Uzun H, Erboga M, Pul M. The effects of hyperbaric oxygen application against cholestatic oxidative stress and hepatic damage after bile duct ligation in rats. J Surg Res 2013;183:146–55.
[79] Huang LT, Tiao MM, Tain YL, Chen CC, Hsieh CS. Melatonin ameliorates bile duct ligation-induced systemic oxidative stress and spatial memory deficits in developing rats. Pediatr Res 2009;65:176–80.
[80] Flores O, Criado M, Sanchez-Rodriguez A, Hidalgo F, Collia F, Lopez-Novoa JM, Esteller A. Relationships between nos2 and ho-1 in liver of rats with chronic bile duct ligation. Hepatol Res: Off J Jpn Soc Hepatol 2005;32:58–65.
[81] Yu J, Chu ES, Wang R, Wang S, Wu CW, Wong VW, Chan HL, Farrell GC, Sung JJ. Heme oxygenase-1 protects against steatohepatitis in both cultured hepatocytes and mice. Gastroenterology 2010;138:694–704. 704 e691.
[82] Yaylak F, Canbaz H, Caglikulekci M, Dirlik M, Tamer L, Ogetman Z, Polat Y, Kanik A, Aydin S. Liver tissue inducible nitric oxide synthase (inos) expression and lipid peroxidation in experimental hepatic ischemia reperfusion injury stimulated with lipopolysaccharide: the role of aminoguanidine. J Surg Res 2008;148:214–23.
[83] Tacke F, Zimmermann HW. Macrophage heterogeneity in liver injury and fibrosis. J Hepatol 2014;60:1090–6.
[84] Stadler K, Bonini MG, Dallas S, Jiang J, Radi R, Mason RP, Kadiiska MB. Involvement of inducible nitric oxide synthase in hydroxyl radical-mediated lipid peroxidation in streptozotocin-induced diabetes. Free Radic Biol Med 2008;45:866–74.
[85] Abraham S, Szabo A, Kaszaki J, Varga R, Eder K, Duda E, Lazar G, Tiszlavicz L, Boros M, Lazar Jr G. Kupffer cell blockade improves the endotoxin-induced microcirculatory inflammatory response in obstructive jaundice. Shock 2008;30:69–74.
[86] Minter RM, Bi X, Ben-Josef G, Wang T, Hu B, Arbabi S, Hemmila MR, Wang SC, Remick DG, Su GL. Lps-binding protein mediates lps-induced liver injury and mortality in the setting of biliary obstruction. Am J Physiol Gastrointest Liver Physiol 2009;296:G45–54.
[87] Miyaso H, Morimoto Y, Ozaki M, Haga S, Shinoura S, Choda Y, Iwagaki H, Tanaka N. Obstructive jaundice increases sensitivity to lipopolysaccharide via tlr4 upregulation: possible involvement in gut-derived hepatocyte growth factor-protection of hepatocytes. J Gastroenterol Hepatol 2005;20:1859–66.
[88] Lai JL, Liu YH, Liu C, Qi MP, Liu RN, Zhu XF, Zhou QG, Chen YY, Guo AZ, Hu CM. Indirubin inhibits lps-induced inflammation via tlr4 abrogation mediated by the nf-kb and mapk signaling pathways. Inflammation 2016.
[89] Carroll TP, Greene CM, Taggart CC, Bowie AG, O'Neill SJ, McElvaney NG. Viral inhibition of il-1- and neutrophil elastase-induced inflammatory responses in bronchial epithelial cells. J Immunol 2005;175:7594–601.
[90] Anitha M, Vijay-Kumar M, Sitaraman SV, Gewirtz AT, Srinivasan S. Gut microbial products regulate murine gastrointestinal motility via toll-like receptor 4 signaling. Gastroenterology 2012;143:1006–1016 e1004.
[91] Bahcecioglu IH, Yalniz M, Ataseven H, Bulbuller N, Kececi M, Demirdag K, Ozercan I, Ustundag B. Tnf-alpha and leptin in experimental liver fibrosis models induced by carbon tetrachloride and by common bile duct ligation. Cell Biochem Funct 2004;22:359–63.
[92] El-Beshbishy HA. Aqueous garlic extract attenuates hepatitis and oxidative stress induced by galactosamine/lipoploysaccharide in rats. Phytother Res: PTR 2008;22:1372–9.